

Model of peak separation in the gamma lightcurve of the Vela pulsar

J. Dyks[★] and B. Rudak[★]

Nicolaus Copernicus Astronomical Center, Rabańska 8, 87-100 Toruń, Poland

Accepted . Received

ABSTRACT

The separation Δ^{peak} between two peaks in the gamma-ray pulse profile is calculated as a function of energy for several polar cap models with curvature-radiation-induced cascades. The Monte Carlo results are interpreted with the help of analytical approximations and discussed in view of the recent data analysis for the Vela pulsar (Kanbach 1999). We find that the behaviour of Δ^{peak} as a function of photon energy ε depends primarily on local values of the magnetic field, B_{local} , in the region where electromagnetic cascades develop. For low values of B_{local} ($< 10^{12}$ G), $\Delta^{\text{peak}}(\varepsilon)$ is kept constant. However, for stronger magnetic fields ($\gtrsim 10^{12}$ G) in the hollow-column model Δ^{peak} decreases with increasing photon energy at a rate dependent on maximum energy of beam particles as well as on viewing geometry. There exists a critical photon energy $\varepsilon_{\text{turn}}$ above which the relation $\Delta^{\text{peak}}(\varepsilon)$ changes drastically: for $\varepsilon > \varepsilon_{\text{turn}}$, in hollow-column models the separation Δ^{peak} increases (whereas in filled-column model it decreases) rapidly with increasing ε , at a rate of ~ 0.28 of the total phase per decade of photon energy. The existence of critical energy $\varepsilon_{\text{turn}}$ is a direct consequence of one-photon magnetic absorption effects. In general, $\varepsilon_{\text{turn}}$ is located close to the high-energy cutoff of the spectrum, thus photon statistics at $\varepsilon_{\text{turn}}$ should be very low. That will make difficult to verify an existence of $\varepsilon_{\text{turn}}$ in real gamma-ray pulsars. Spectral properties of the Vela pulsar would favour those models which use low values of magnetic field in the emission region ($B_{\text{local}} \lesssim 10^{11}$ G) which in turn implies a constant value of the predicted Δ^{peak} within *EGRET* range.

Key words: pulsars: general – pulsars: individual: PSR B0833–45 – gamma-rays: observations – gamma-rays: theory.

1 INTRODUCTION

Two prominent peaks are a characteristic feature of gamma-ray pulse shapes in the three brightest out of seven gamma-ray pulsars detected so far: Crab (PSR B0531+21), Vela (PSR B0833-45), and Geminga (J0633+1746). Phase separation between the two peaks is very large in each case, in the range between 0.4 and 0.5 (e.g. Fierro, Michelson & Nolan 1998). The separation, which we denote by Δ^{peak} , was determined with photons from the entire energy range of *EGRET*.

Kanbach (1999) suggested that the separation Δ^{peak} in Vela might be energy dependent. The effect would be of the order of a few percent or less. The plot of the phase separation against energy (fig.2 of Kanbach 1999) shows that Δ^{peak} decreases by about 5% over 20 energy intervals covering the range between ~ 50 MeV and ~ 9 GeV. The scatter of points is, however, large enough for this result still to be

consistent with the separation staying at a constant level of 0.43, especially when one rejects two energy intervals: of the lowest and the highest value.

Such effects as suggested by Kanbach can be justified qualitatively, at least within polar cap scenarios. Their origin may be different at different energy ranges, and their magnitude may vary as well. For example, Miyazaki & Takahara (1997) found dramatic changes in peak-to-peak phase separation due to magnetic absorption effects in their attempts to model the Crab pulse shapes. Their numerical calculations were performed with low photon energy resolution for a model with homogeneous polar cap, and instant acceleration.

This new aspect of studying the HE properties of pulsars is potentially attractive. The problem of poor photon statistics should become less essential with future high-sensitivity missions like *GLAST*. Then any well established empirical relation between the phase separation Δ^{peak} and the photon energy ε (including $\Delta^{\text{peak}} = \text{const}$) may help to

[★] E-mail: jinx@ncac.torun.pl (JD); bronek@camk.edu.pl (BR)

discriminate in favour of some particular models of pulsar activity.

In this context we present a model of the peak-to-peak phase separation in the gamma-ray lightcurve of Vela and confront it with the results of Kanbach (1999). Our aim is to present properties of $\Delta^{\text{peak}}(\zeta)$ predicted by the polar cap model with curvature (CR) and synchrotron (SR) radiation being dominant emission mechanisms. This is an extension of the preliminary results of Dyks, Rudak & Bulik (2000). In section 2 we outline the model and introduce the input parameters for which Monte Carlo simulations were performed. Section 3 describes the numerical results and offers their interpretation; conclusions follow in section 4.

2 THE MODEL

The presence of two peaks with large (0.4 - 0.5) phase separation in gamma-ray lightcurves within single polar cap models requires a nearly aligned rotator (e.g. Daugherty & Harding 1994) where the following three characteristic angles are to be of the same order: α - the angle between the spin axis Ω and the magnetic moment μ , ϑ_γ - the opening angle between the direction of the gamma-ray emission and μ , and ζ - the angle between Ω and the line of sight. For a canonical polar cap and instant electron acceleration, ϑ_γ roughly equals $0.02/\sqrt{P}$ radians only (where P denotes a spin period). To avoid uncomfortably small characteristic angles, Daugherty & Harding (1996), postulated that primary electrons come from extended polar caps, and with the acceleration occurring at a height h of several neutron-star radii R_{ns} . The latter assumption may be supported by the results of Harding & Muslimov (1998) who investigated in a self-consistent way particle acceleration by the electrostatic field due to field-line curvature (Arons 1983) and inertial frame dragging effect (Muslimov & Tsygan 1992). Harding & Muslimov found that a stable accelerator, with double pair-formation-front controlled by curvature radiation, is possible at a height of about 0.5 to 1 stellar radii. Here we use a polar cap model combined with the assumption of a nearly aligned rotator. Most ingredients of the pc-model come from Daugherty & Harding (1982). Geometry of the magnetic field of a neutron star is assumed to be well described by a static, axisymmetric dipole.

Within a given polar cap (pc) model with a fixed value of α there are two possible values of viewing angle ζ resulting in an identical peak separation Δ^{peak} (defined as a fraction of 2π) but with a reversed order of the two peaks (in terms of a leading peak, and then a trailing peak). Fig. 1 illustrates the ambiguity in the definition of a double-peak pulse. A simple geometrical relation connects the three angles of interest - α , ζ and ϑ_γ - to the phase separation Δ^{peak} :

$$\cos \vartheta_\gamma = \cos \delta \sin \alpha \sin \zeta + \cos \alpha \cos \zeta, \quad (1)$$

(eg. Ochelkov & Usov 1980), where $\delta = \pi \Delta^{\text{peak}}$ for ζ_{large} , and $\delta = \pi(1 - \Delta^{\text{peak}})$ for ζ_{small} . This relation holds as far as aberration of photon propagation due to rapid rotation is neglected.

Throughout the paper we always take the case of the larger ζ in each model (4 models are considered). Its value ($\zeta_{\text{large}} = 3.75, 4.5, 15.$, and 3.65 degrees for models A, B,

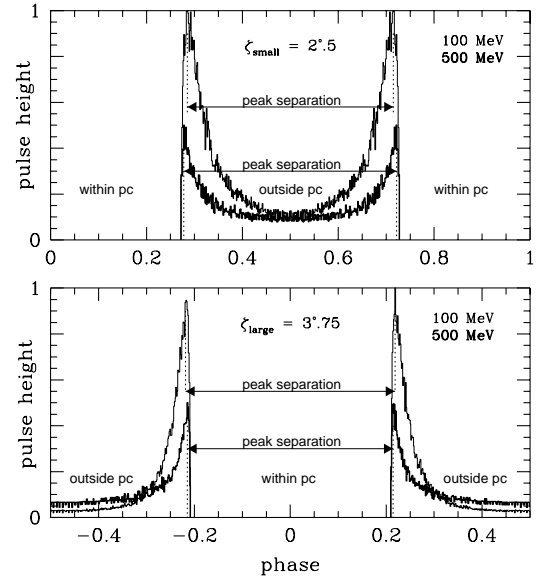


Figure 1. The double-peak pulses at 100 MeV (thin line) and 500 MeV (thick line) calculated for model A. Depending on viewing angle ζ between the spin axis Ω and the line of sight each single polar cap model yields two types of double-peak pulses. The upper and lower panels show the pulses for two values of the angle ζ : $\zeta_{\text{small}} = 2.5$ deg and $\zeta_{\text{large}} = 3.75$ deg, respectively.

C, and D, respectively) along with our choice for the angle α (see Table 1) is to yield the separation $\Delta^{\text{peak}} = 0.43$ at 300 MeV.

The dominant HE emission process is the curvature radiation (CR) by ultrarelativistic beam particles (primary electrons which leave the polar cap), followed by magnetic pair production with the subsequent synchrotron emission (SR). Our numerical code to follow the cascades induced by beam particles is based on Daugherty & Harding (1982), and takes advantage of the following approximations relevant to the problem of directional and spectral distributions of the photons: The curvature photons are emitted tangentially to the local magnetic field direction in a frame rotating with the star. The created e^\pm -pairs are assumed to follow the directions of their parent CR photons and they share the photons' energy equally (for justification see Daugherty & Harding 1983). The synchrotron photons are emitted perpendicularly to the local magnetic field direction in a frame comoving with electron/positron center of gyration. The pairs are assumed not to change their position on the field line when radiating (for magnetic field strengths considered here, energy-loss length scales due to SR are of the order of 10^{-6} cm). The emergent high-energy spectrum is a superposition of CR and SR. We follow Rudak & Dyks (1999) to calculate detailed broad band energy spectra of the high-energy emission.

Beam particles are injected along magnetic field lines into the magnetosphere either from the outer rim of the polar cap (hollow cone column) or from the entire polar cap surface (filled column). We use two simple models for their acceleration to ultrarelativistic energies: 1) instant acceleration and 2) acceleration due to a uniform longitudinal electric field \mathcal{E} over a scale height Δh . The pulse

Table 1. Model parameters.

	B_{pc}	α	h_{init}	θ_{init}	
	$[10^{12} \text{ G}]$	[deg]	$[R_{\text{ns}}]$	$[\theta_{\text{pc}}]$	primary electrons
Model A	1.0	3.0	0.0	1.0	$E_{\text{init}} = 8.68 \text{ TeV, no acceleration}$
Model B	1.0	5.0	1.0	1.0	$E_{\text{init}} = 20.0 \text{ TeV, no acceleration}$
Model C	3.0	10.0	2.0	2.0	$E_{\text{init}} = 0.5 \text{ MeV, acceleration (see eq.(2))}$ with $V_0 = 1.5 \times 10^{13} \text{ Volts}$
Model D	1.0	3.0	0.0	$[0, 1]$	$E_{\text{init}} = 8.68 \text{ TeV, no acceleration}$

shapes as a function of photon energy were calculated numerically for four sets of initial parameters (hereafter called models A, B, C and D). Table 1 features most important model parameters. In models A and B the primary electrons are distributed evenly along a hollow cone formed by the magnetic field lines from the outer rim of a canonical polar cap, i.e. with a magnetic colatitude $\theta_{\text{init}} = \theta_{\text{pc}}$, where $\theta_{\text{pc}} \simeq (2\pi R_{\text{ns}}/cP)^{1/2}$ radians at the stellar surface level ($h = 0$). The beam particles are injected at a height h_{init} with some initial ultrarelativistic energy E_{init} (listed in Table 1) and no subsequent acceleration takes place. The main difference between models A and B is due to different values of h_{init} (equal to 0 and 1 R_{ns} respectively) which result in different locations of origin of secondary particles. Changing these locations is an easy way to modify spectral properties of emergent radiation and enables to change (preferably - to increase) the angle α as constrained by the observed energy-averaged peak separation $\Delta^{\text{peak}} \approx 0.43$ (Kanbach 1999). In model C we assume $\theta_{\text{init}} = 2\theta_{\text{pc}}$. The primaries are injected at $h_{\text{init}} = 2R_{\text{ns}}$ with $E_{\text{init}} = mc^2$ and undergo acceleration by a longitudinal electric field \mathcal{E} present over a characteristic scale height $\Delta h = 0.6 R_{\text{ns}}$, resulting in a total potential drop V_0 :

$$\mathcal{E}(h) = \begin{cases} V_0/\Delta h, & \text{for } h_{\text{init}} \leq h \leq (h_{\text{init}} + \Delta h) \\ 0, & \text{elsewhere.} \end{cases} \quad (2)$$

For comparison, we considered model D with a uniform electron distribution over the entire polar cap surface (i.e. $\theta_{\text{init}} \in [0, \theta_{\text{pc}}]$). All its remaining features are identical to model A.

The values of E_{init} in models A, B and D, and the potential drop V_0 in model C were chosen to yield similar number of secondary pairs — about 10^3 per beam particle. In all cases the spin period of the Vela pulsar $P = 0.089 \text{ s}$ was assumed.

3 RESULTS

General properties of the function $\Delta^{\text{peak}}(\varepsilon)$ may be described in short in the following way: In the low-energy range (i.e. below a few GeV) the peak separation either remains constant with the increasing photon energy (Models B, C, and D) or slightly decreases (Model A). In either case, however, the slope of Δ^{peak} versus ε looks consistent with the results of Kanbach (1999). Then, around a few GeV there exists a critical energy $\varepsilon_{\text{turn}}$, at which the separation Δ^{peak} undergoes a sudden turn: in the high-energy domain (i.e. for $\varepsilon > \varepsilon_{\text{turn}}$) it increases in our hollow-column models (A, B, and C), whereas it decreases in the filled-column model (D), at a rate ~ 0.28 phase per decade of photon energy. The ex-

istence of $\varepsilon_{\text{turn}}$ is a direct consequence of magnetic absorption ($\gamma \mathbf{B} \rightarrow \mathbf{e}^{\pm}$) in the magnetosphere (see also Miyazaki & Takahara 1997). [Note, that $\varepsilon_{\text{turn}}$ is not equivalent to a high-energy cut-off in a spectrum due to the magnetic absorption].

The dependence of peak separation upon photon energy for all four models is presented in Fig. 2 (upper panels).

To understand why the slope in the low-energy domain ($\varepsilon < \varepsilon_{\text{turn}}$) is different in different models, we will now present several factors which are of interest in this respect.

Let us start with possible consequences of the orientation on $\Delta^{\text{peak}}(\varepsilon)$ in this context, i.e. with the choice of the angles α and ζ . For a given emission pattern in a frame of magnetic dipole rotating with the star and for a set of values of angles α and ζ fulfilling the condition $\Delta^{\text{peak}}(300 \text{ MeV}) = 0.43$, a line of view can cross the hollow cone of emission at different impact angles. Let us estimate how geometry alone would affect the relations $\Delta^{\text{peak}}(\varepsilon)$ shown in Fig. 2. We neglect aberration of photon propagation due to rotation when calculating directional emission pattern as seen from some inertial observer frame. For Δ^{peak} staying close to 0.5 (roughly between ~ 0.3 and ~ 0.7) $\cos(\pi \Delta^{\text{peak}}) \simeq \frac{\pi}{2} - \pi \Delta^{\text{peak}}$, the value of $\cos \vartheta_{\gamma}$ is approximately proportional to Δ^{peak} with a constant of proportionality equal to $-\pi \sin \alpha \sin \zeta$. Moreover, for a radiating particle sliding along a dipolar field line with the dipole constant $k = r \sin^{-2} \theta$ (r, θ are the coordinates of the particles in the dipolar frame), one can link the opening angle ϑ_{γ} with a radial position r of the particle:

$$\cos \vartheta_{\gamma} = \frac{2 - 3 \frac{r}{k}}{\sqrt{4 - 3 \frac{r}{k}}}. \quad (3)$$

Since in polar cap models $\frac{r}{k} \ll 1$, the right-hand side of eq. (3) can be approximated by $\cos \vartheta_{\gamma} \simeq 1 - \frac{9}{8} \frac{r}{k}$ which along with eq.(1) gives

$$r \simeq \frac{8}{9} \pi a \Delta^{\text{peak}} + b \quad (4)$$

where

$$a \equiv k \sin \alpha \sin \zeta,$$

and

$$b \equiv \frac{8}{9} k \left(1 - \frac{\pi}{2} \sin \alpha \sin \zeta - \cos \alpha \cos \zeta \right).$$

The slope of the relation $\Delta^{\text{peak}}(\varepsilon)$ is a combination of two factors: 1) viewing geometry and 2) directional and spectral changes in the radiation yielding the peaks with increasing radial coordinate r :

$$\frac{d\Delta^{\text{peak}}}{d\varepsilon} = \frac{d\Delta^{\text{peak}}}{dr} \cdot \frac{dr}{d\varepsilon}. \quad (5)$$

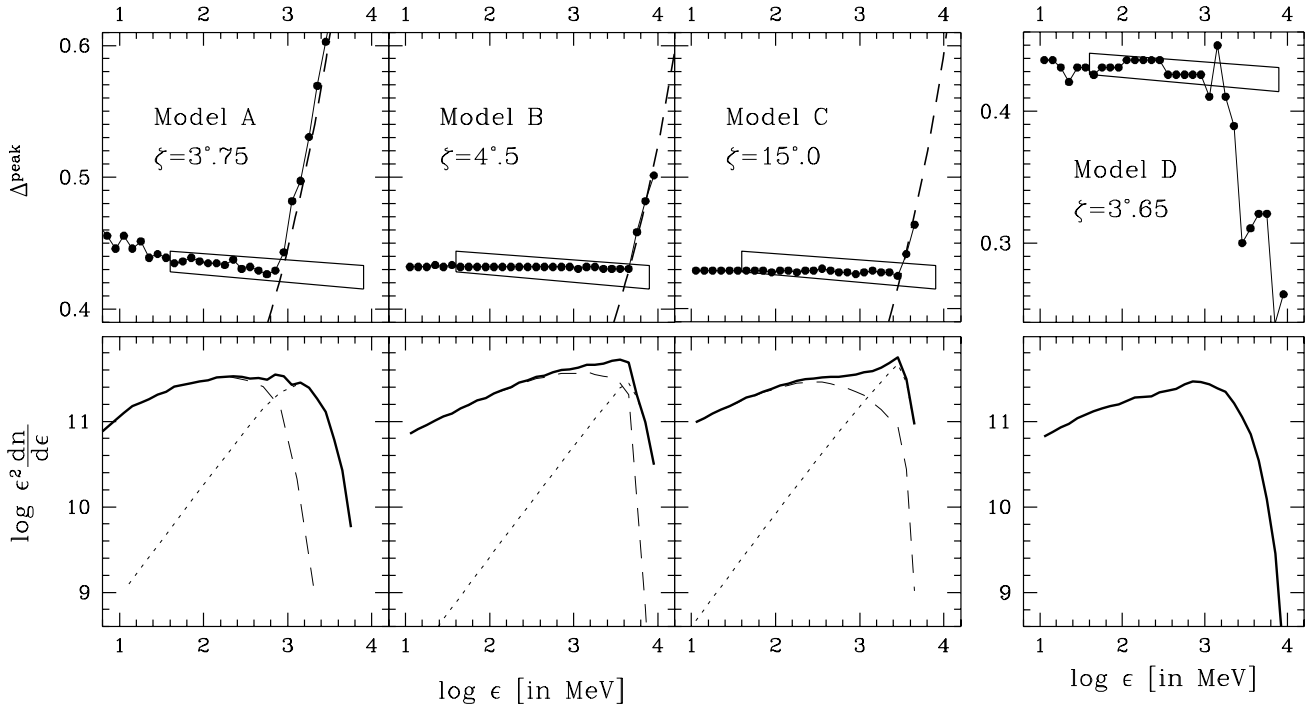


Figure 2. Upper panels: Phase separation Δ^{peak} versus photon energy ε of the emission peaks found with Monte Carlo calculations for models A, B, C and D (dots). The overall observational trend, taking into account a substantial scatter of points (see fig.2, middle panel, of Kanbach 1999), is marked schematically for reference in all four panels as a parallelogram. The assumed values of ζ - the angle between Ω and the line of sight - are also indicated. The steep dashed lines in the three left-hand side panels (hollow-column models) are the approximate analytical solutions for Δ^{peak} determined by magnetic absorption effects ($\gamma\mathbf{B} \rightarrow e^\pm$). They reproduce the Monte Carlo results with good accuracy in the high energy limit (the GeV domain). Lower panels: Energy output per logarithmic energy bandwidth at the first peak as a function of photon energy ε for models A, B, C and D. The synchrotron (long dashed) and the curvature (short dashed) components are marked for models A, B, and C. [Note: these are not instantaneous spectra.] Units on the vertical axis are arbitrary.

Any changes in viewing geometry (i.e. the angles α and ζ) will affect the slope $d\Delta^{\text{peak}}/d\varepsilon$ via $d\Delta^{\text{peak}}/d\varepsilon = \frac{9}{8\pi a}$, the latter being calculated from eq.(4). For example, for models A and B the parameter a equals $1.46R_{\text{ns}}$ and $2.91R_{\text{ns}}$, respectively. Should $dr/d\varepsilon$ be identical for these two models, the slope in model A would be about two times bigger than in model B. Fig. 2 (upper panels) does not show any such effects: the slope in model B is ≈ 0 for $\varepsilon < \varepsilon_{\text{turn}}$. This is because the viewing geometry effects are dwarfed by differences in directional and spectral properties of the radiation in these models.

To analyse directional and spectral properties of the peak emission it is instructive to begin with a simplified, one-component model. Suppose that the only contribution to the emission is due to optically thin CR, i.e. both magnetic absorption and synchrotron emission by secondary pairs created due to this absorption are neglected. Numerical simulations of this case (not included in this paper) show that the peak separation in such a case, which we denote as $\Delta_{\text{cr}}^{\text{peak}}$, stays constant as a function of ε for the models with instant acceleration (A, B, D), while it increases with increasing ε for model C (acceleration over Δh) at a rate dependent on the electron acceleration rate. The former case can be understood by arguing that energy $E = \gamma mc^2$ of the electron decreases monotonically from its starting value E_{init} , while its radius of curvature ρ_{cr} increases. Recalling the properties

of the curvature continuous spectrum due to a single particle (e.g. Landau & Lifshitz 1973) this makes the contribution to the spectrum per unit distance by the electron to be the highest one just at the initial altitude h_{init} . In consequence, the contribution to the spectrum per unit phase angle by a bundle of electrons moving along a set of open field lines is the highest one at h_{init} . Therefore, it is the opening angle of the CR photons at h_{init} which fixes the phase separation $\Delta_{\text{cr}}^{\text{peak}}$ of the two peaks regardless the photon energy. In the latter case the qualitative behaviour of $\Delta_{\text{cr}}^{\text{peak}}(\varepsilon)$ can be understood by assuming that the phase of the pulse peak at a given photon energy ε is approximately determined by such altitude at which accelerated electrons reach the energy γmc^2 which satisfies the condition $0.29 \varepsilon_{\text{cr}}(\gamma, \rho_{\text{cr}}) \approx \varepsilon$, where $\varepsilon_{\text{cr}} = \frac{3}{2}c\hbar\gamma^3\rho_{\text{cr}}^{-1}$ is a characteristic energy of the CR spectrum and ρ_{cr} is a local radius of curvature; both γ and ρ_{cr} are functions of altitude h .

We now relax these two simplifications and present the consequences. First, the inclusion of magnetic absorption results in a strong response of $\Delta_{\text{cr}}^{\text{peak}}$ at highest photon energies - between some critical energy $\varepsilon_{\text{turn}}$ and the high-energy cutoff, as mentioned in the first paragraph. This effect will be addressed in the final part of this section. Second, adding up synchrotron component (SR) due to e^\pm pairs changes the properties of high-energy emission for $\varepsilon < \varepsilon_{\text{turn}}$ (i.e. below a few GeV) significantly. Most notable is the domination of SR

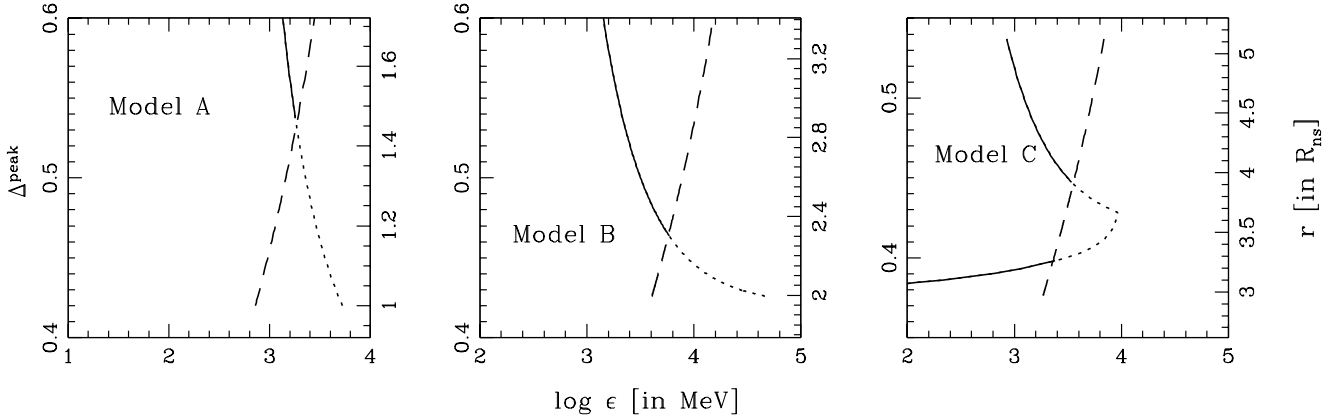


Figure 3. Phase separation Δ^{peak} versus photon energy ε corresponding to the directions of propagation of curvature photons emitted by electrons located on annuli (each annulus corresponds to a given radial coordinate and a dipolar constant; it translates into Δ^{peak} for a fixed set of angles between the spin axis Ω , the magnetic moment μ , and the line of sight). The curvature photons are here assumed to have a characteristic energy $\varepsilon_{\text{cr}} = 1.5c\hbar\gamma_{\text{el}}^3\rho_{\text{cr}}^{-1}$ (the dimensionless energy γ_{el} of the electrons as well as the local radius of curvature ρ_{cr} change along electron's trajectory in a model dependent way). Dashed lines (as in Fig. 2, upper panels) represent the limiting energy ε_{esc} of curvature photons for which the magnetosphere becomes opaque. Photons located to the right of the dashed line in each panel convert into e^\pm pairs. This part of Δ^{peak} vs. ε is shown as dotted line. The pairs produce the synchrotron spectral component which in turn determines the character of Δ^{peak} vs. ε in the low-energy domain (see Fig. 2, upper panels). Note a wide range of Δ^{peak} values for which curvature photons are absorbed in Model A, in contrast to Models B and C.

over CR in terms of intensity. The total energy output per logarithmic energy bandwidth at the first peak as a function of photon energy ε for models A, B, C and D is presented in Fig. 2 (lower panels). Both components – SR and CR – are marked schematically to show their relative importance. Consequently, Δ^{peak} is affected by directional and spectral properties of the SR emission.

The behaviour of Δ^{peak} is shown in Fig. 2 (upper panels). Its slight decrease with increasing ε (model A) or no change at all (models B, C, and D) – is due to a combination of factors which determine the directional and spectral properties of SR. These include energy and pitch angle distributions of secondary e^\pm pairs, as well as their vertical spread within the magnetosphere combined with a strength of the local magnetic field. These factors change from one model to another:

Model A - In strong local magnetic fields ($B_{\text{local}} \approx 10^{12}$ G), efficient pair production requires lower electron energies than in a low-field case (like in model B). The production occurs over a wider range of altitudes. Consequently, the spectrum of SR contributed locally by the pairs evolves considerably over this range of altitudes. Lorentz factors of gyration γ_\perp are of low values (of the order of $mc^2/(15\varepsilon_B)$, where $\varepsilon_B \equiv mc^2B_{\text{local}}/B_{\text{crit}}$). The resulting local SR spectra are, therefore, very narrow (see also the lower panel of fig. 1 in Rudak & Dyks 1999): they spread between the (local) characteristic SR energy ε_{sr} and the (local) cyclotron turnover energy $\varepsilon_{\text{ct}} = 1.5\varepsilon_B/\sin\psi$ (where ψ is the pitch angle) which roughly satisfy $\varepsilon_{\text{sr}}/\varepsilon_{\text{ct}} \approx \gamma_\perp^2$, and the ratio does not exceed 10^3 in model A. With increasing height (therefore, with decreasing B_{local}) both ε_{sr} and ε_{ct} move towards lower and lower values. The final effect of this softening is then a notable decrease of Δ^{peak} with increasing photon energy (Fig. 2, upper panel, Model A). In even stronger local magnetic fields (but not exceeding B_{crit}) the rate of decrease of Δ^{peak} with increasing ε may be much larger,

because e^\pm -pairs are produced with extremely low γ_\perp and synchrotron/cyclotron photons emitted at any altitude concentrate near the local cyclotron energy ε_B .

Model B - When cascades are to develop in a relatively weak magnetic field, $B_{\text{local}} \lesssim 10^{11}$ G, very high electron energy E_{init} is required. The high value of E_{init} means rapid CR cooling which brings the electron energy quickly below the level required for pair production. Curvature photons become too soft for pair creation via magnetic absorption very quickly after injection. The bulk of pairs is created by electrons with their energies confined to a narrow range at E_{init} and consequently the SR component originates within a narrow range of magnetospheric altitudes (radial positions r). The resulting Δ^{peak} does not change with photon energy ε .

The difference between model A and B in radial extension r of the regions of origin of curvature photons which are absorbed, producing pairs and eventually SR, is presented in Fig. 3 (right-hand vertical axes). The difference is more appealing when presented in terms of Δ^{peak} (left-hand vertical axes).

Model C - After initial stage of linear acceleration, the electrons enter a regime of ‘radiation reaction limited acceleration’. Over a considerable range of altitudes ($3.3R_{\text{ns}} \lesssim r \lesssim 3.6R_{\text{ns}}$) the electrons’ energy remains approximately constant and so does the pair production efficiency (it is equal to $\sim 4 \cdot 10^{-3}$ pairs per centimetre of the primary electron path). In such conditions, any evolution of the SR-spectrum over this range might affect Δ^{peak} as a function of ε . Nevertheless, no significant changes occur in $\Delta^{\text{peak}}(\varepsilon)$. This is because a single-particle SR-spectrum almost does not change its shape within the range of altitudes with stable, strong pair production. The balance between the acceleration rate and the CR-cooling rate stabilizes ε_{cr} as well as ε_{sr} . Any spectral changes of SR in its low-energy part, nearby ε_{ct} , are

not relevant in the context of gamma-rays, since they occur near 100 keV, i.e. well below the energy range of *EGRET*.[†] Model D (a uniform distribution of primary electrons over the polar cap but otherwise identical to model A) - the final effect does not resemble the decrease of Δ^{peak} with increasing photon energy found for model A. Apart from numerical fluctuations (see Fig. 2, upper panel) the separation Δ^{peak} remains approximately constant as a function of ε .

Finally, let us discuss the inclusion of magnetospheric opacity due to $\gamma\mathbf{B} \rightarrow \mathbf{e}^\pm$. This effect becomes important above ~ 1 GeV, where most power is due to CR in all models. In this regime the position of each peak in the pulse is determined by magnetic absorption, and this results in a strong response of Δ^{peak} between $\varepsilon_{\text{turn}} \gtrsim 1$ GeV and a high-energy cutoff: At $\varepsilon = \varepsilon_{\text{turn}}$ the separation Δ^{peak} undergoes a sudden turn and starts increasing (or decreasing) rapidly for $\varepsilon > \varepsilon_{\text{turn}}$. For the hollow-column models (A, B and C) the photons in both peaks of a pulse come from low magnetospheric altitudes with narrow opening angles. When ε is high enough these photons will be absorbed. Photons which now found themselves in the ‘new’ peaks come from higher altitudes (the magnetosphere is transparent to them) and have wider opening angles. In other words, inner parts of the ‘original’ peaks in the pulse will be eaten-up and the gap between the peaks, i.e. the peak separation Δ^{peak} , will increase (Fig.2). Our Monte Carlo results for Δ^{peak} at $\varepsilon > \varepsilon_{\text{turn}}$ may be reproduced with good accuracy by a simple analytical solution of $\tau_{\gamma B} \geq 1$ which has to be combined with eq.(4). The requirement $\tau_{\gamma B} \geq 1$ is particularly simple (with some well known approximations being used) since it refers to a photon created with a momentum tangential to local dipolar magnetic field line at a height h above the neutron star surface (at radial coordinate $r = h + R_{\text{ns}}$). The photon will undergo magnetic absorption (to be more precise, with a probability of $[1 - \exp(-\tau_{\gamma B})]$) if its energy ε satisfies the following condition:

$$\varepsilon > \varepsilon_{\text{esc}} = 7.6 \cdot 10^2 \left(\frac{P}{0.1\text{s}} \right)^{1/2} \left(\frac{B_{\text{pc}}}{10^{12} \text{ G}} \right)^{-1} \left(\frac{r}{R_{\text{ns}}} \right)^{5/2} \text{ MeV}, \quad (6)$$

(cf. eq. 11 in Bulik et al. 1999). This formula is valid for hollow-column models but may be used for any dipolar field line (the factor $P^{1/2}$ comes just from choosing the outer rim of a polar cap to be the site of field-line footpoints). Although the pulsar spin (which leads to an aberration and a slippage of magnetic field under the photon’s path) has been neglected in derivation of eq. (6), the formula gives ε_{esc} in excellent agreement with Monte Carlo method for the emission regions placed up to several R_{ns} above the surface and rotation periods typical for strong-field pulsars ($\gtrsim 10^{-2}$

[†] The behaviour of SR in its low-energy part (i.e. in hard X-rays) may then lead to increase of Δ^{peak} in the hard X-ray domain in comparison to Δ^{peak} in the gamma-rays. Assuming alternative to our choice definition of Δ^{peak} , with ζ_{small} (see Section 2), the behaviour of Δ^{peak} would be a mirror-reflection of our case. Then this effect might explain low value of Δ^{peak} within the 2–30 keV range found by Strickman, Harding & deJager (1975) in *RXTE* data of Vela. Moreover, below 2 keV the synchrotron component in the model spectrum drops below the level of CR-emission, and the value of Δ^{peak} as for the gamma-rays is expected to be resumed there.

s). One may look at the eq.(6) as the condition for a radius of escape r_{esc} at a given energy ε . Photons of energy ε will escape the magnetosphere only if they are emitted at $r \geq r_{\text{esc}}$ which satisfies $\varepsilon_{\text{esc}}(r) \geq \varepsilon$. The radial coordinate $r_{\text{esc}}(\varepsilon)$ has to be combined now with eq.(4) to give Δ^{peak} relevant for the ‘magnetic absorption’ regime. This analytical Δ^{peak} is shown as dashed lines in Fig.2 (upper panels) and in Fig.3, whereas the filled dots are the Monte Carlo results. This branch of solution intersects the horizontal line set by $\Delta^{\text{peak}} = 0.43$ at $\varepsilon_{\text{turn}} \simeq 0.9, 4.5$, and 3 GeV for models A, B, and C, respectively.

For model D, with a uniform distribution of primary electrons over the polar cap (but otherwise identical to model A) the changes of Δ^{peak} above $\varepsilon_{\text{turn}}$, occur in the opposite sense. Unlike in previous models, here both peaks of the pulse are formed by photons emitted tangentially to magnetic field lines attached to the polar cap at some opening angle $\theta_{\text{init}} < \theta_{\text{pc}}$. These photons are less attenuated than those coming from a hollow-column, and in consequence the peak separation drops. A similar behaviour was obtained by Miyazaki & Takahara (1997), in their model of a homogeneous polar-cap.

We have also investigated the behaviour of $\Delta^{\text{peak}}(\varepsilon)$ above $\varepsilon_{\text{turn}}$ for other distributions of primary electrons over the polar cap. We have considered intermediate cases between models A and D, (i.e. with a uniform coverage of only an outer part of the polar cap area between some inner radius $r_{\text{in}} < r_{\text{pc}}$ and the polar cap radius r_{pc}), and models with uniformly filled interior of the polar cap surface but with increased electron density along the polar cap rim (cf. Daugherty & Harding 1996). We conclude that regardless the actual shape of the active part (i.e. ‘covered’ with primary electrons) of the polar cap (either an outer rim, or an entire cap, or a ring, or entire cap/ring + increased rim density), one does expect in general strong changes in the peak separation to occur at photon energies close to high-energy spectral cutoff due to magnetic absorption.

A word of technical comment seems to be appropriate for $\Delta^{\text{peak}} = 0.43$ at ~ 300 MeV. It appears that a technique adopted by Kanbach (1999) of fitting the observed pulse shapes with asymmetric Lorentz profiles tends to overestimate the true value of Δ^{peak} by a few thousandth parts of phase. Therefore the actual value may be closer to 0.42 than 0.43 (Maurice Gros, private communication). Nonetheless, this shift in Δ^{peak} does not change any conclusions of this work.

4 SUMMARY

In this paper we addressed a recent suggestion of Kanbach (1999) that peak separation Δ^{peak} in the double-peak gamma-ray pulses of the Vela pulsar may monotonically decrease with increasing photon energy at a rate ~ 0.025 phase per decade in energy over the range 50 MeV to 9 GeV. We calculated gamma-ray pulses expected in polar-cap models with magnetospheric activity induced by curvature radiation of beam particles. Two types of geometry of magnetospheric column above the polar cap were assumed: a hollow-column associated with an outer rim of the polar cap and a filled column associated with a uniform polar cap. Four models were considered with two scenarios for the acceleration of beam particles. Pulsed emission in the models was a super-

position of curvature radiation due to beam particles and synchrotron radiation due to secondary e^\pm pairs in magnetospheric cascades. The changes in the peak separation were investigated with Monte Carlo numerical simulations.

We found that regardless the differences in the models, the peak separation Δ^{peak} below a few GeV, where the emission is dominated by synchrotron component, is either a weak decreasing function of photon energy ε , or remains constant. Both variants may be considered to be in agreement with the results of Kanbach (1999) for the latter are affected by large statistical errors. A particular behaviour of Δ^{peak} depends on a combination of several factors, including strength of magnetic field in the region of pair formation and model of electron acceleration (both of which determine spectral and directional properties of the radiation at different altitudes), as well as viewing geometry. Essentially, in strong fields, $B_{\text{local}} \gtrsim 10^{12}$ G, Δ^{peak} decreases with increasing photon energy ε , whereas for $B_{\text{local}} < 10^{12}$ G, the peak separation Δ^{peak} stays at a constant level.

Moreover, we found that due to the magnetic absorption ($\gamma\mathbf{B} \rightarrow e^\pm$) there exists a critical energy $\varepsilon_{\text{turn}}$ at which the peak separation Δ^{peak} makes an abrupt turn and then changes dramatically for $\varepsilon > \varepsilon_{\text{turn}}$. It increases in the hollow-column models (A, B, and C) and decreases in the filled-column model (D), at a rate ~ 0.28 phase per decade of photon energy. The numerical behaviour of Δ^{peak} in this regime in the hollow-column models was easily reproduced to high accuracy with a simple analytical model of magnetospheric transparency for a photon of energy ε , and its momentum tangential to local dipolar magnetic field line at a site of its origin. An exact value of $\varepsilon_{\text{turn}}$ is model-dependent but it is confined to a range between ~ 0.9 GeV and ~ 4.5 GeV.

To find such a hypothetical turnover of Δ^{peak} in real observational data would require, however, high-sensitivity detectors, since for $\varepsilon > \varepsilon_{\text{turn}}$ the expected flux of gamma-rays drops significantly. If detected, this turnover would be an important signature of polar cap activity in gamma-ray pulsars. It would support the notion that high-energy cut-offs in gamma-ray spectra of pulsars are due to magnetic absorption.

The CR-induced cascades models, like those considered in this work, are not the only possibility for nearly aligned rotators to produce double-peak pulses with large phase separations. There exists an alternative class of models - with pair cascades above polar cap induced by magnetic inverse Compton scatterings (ICS) of primary electrons in the field of soft photons from the stellar surface - proposed in a series of papers (e.g. Sturmer & Dermer 1994, Sturmer et al. 1995). In particular, Sturmer et al. (1995) present the detailed Monte Carlo model spectra of the Vela pulsar. They also present pulse profiles at a fixed energy of 50 MeV (for several viewing angles) but no word of comment is given regarding the problem of Δ^{peak} versus photon energy. We expect the outcome to be qualitatively similar to our results. First, the scatterings take place mostly within a very limited height above the polar cap surface (below $h \sim R_{\text{pc}}$) and the preferred directions of propagation of the ICS photons will be fixed by magnetic field lines just above the surface. Therefore, Δ^{peak} due solely to ICS photons should stay constant for a wide range of energy. Inclusion of synchrotron photons due to pairs is unlikely to notably affect Δ^{peak} unless the pair formation front is vertically more extended than for

CR-induced cascades. Second, some turnover point at $\varepsilon_{\text{turn}}$ not exceeding 1 GeV should be present due to magnetic absorption. The behaviour of Δ^{peak} for $\varepsilon > \varepsilon_{\text{turn}}$ should roughly follow the dashed lines in Fig. 2 (upper panel) and Fig. 3 as long as the assumption about photons (which are to be absorbed) propagating tangentially to local dipolar magnetic field line at their site of origin remains valid for majority of ICS photons.

To verify this qualitative picture would, however, require detailed numerical calculations.

ACKNOWLEDGEMENTS

This work has been financed by the KBN grants 2P03D-01016, and 2P03D-02117. Support from Multiprocessor Systems Group at Nicholas Copernicus University's Computer Centre in providing facilities for the time/memory-consuming Monte Carlo calculations is appreciated. We are grateful to Gottfried Kanbach and Maurice Gros for valuable discussions on processing and analysis of high-energy data for the Vela pulsar. We thank the anonymous referee for bringing our attention to the paper by Sturmer et al. (1995).

REFERENCES

Arons J., 1983, *ApJ*, 266, 215
 Dyks J., Rudak B., Bulik T., 2000, in Proc. 19th Texas Symposium, in the press
 Daugherty J. K., Harding A. K., 1982, *ApJ*, 252, 337
 Daugherty J. K., Harding A. K., 1983, *ApJ*, 273, 761
 Daugherty J. K., Harding A. K., 1994, *ApJ*, 429, 325
 Daugherty J. K., Harding A. K., 1996, *ApJ*, 458, 278
 Fierro J. M., Michelson P. F., Nolan P. L., Thompson D. J., 1998, *ApJ*, 494, 734
 Harding A. K., Muslimov A. G., 1998, *ApJ*, 508, 328
 Kanbach G., 1999, in Proc. 3rd INTEGRAL Workshop, Astrophysical Letters and Communications, 38, 17
 Landau L. D., Lifshitz E. M., 1977, *The Classical Theory of Fields*, PWN, Warsaw
 Miyazaki J., Takahara F., 1997, *MNRAS*, 290, 49
 Muslimov A. G., Tsygan A. I., 1992, *MNRAS*, 255, 61
 Ochelkov Y. P., Usov V. V., 1980, *Ap.Sp.Sci.*, 69, 439
 Rudak B., Dyks J., 1999, *MNRAS*, 303, 477
 Strickman M. S., Harding A. K., deJager O. C., 1999, *ApJ*, 524, 373
 Sturmer S.J., Dermer C.D., 1994, *ApJ*, 420, L79
 Sturmer S. J., Dermer C. D., Michel F. C., 1995, *ApJ*, 445, 736

This paper has been produced using the Royal Astronomical Society/Blackwell Science L^AT_EX style file.